Preprints of the 19th World Congress
The International Federation of Automatic Control
Cape Town, South Africa. August 24-29, 2014

BESS Control Strategies for Participating in Grid Frequency Regulation

Bolun Xu * **Alexandre Oudalov** * **Jan Poland** *
Andreas Ulbig ** **Göran Andersson** **

* *ABB Switzerland Ltd., CH-5405 Dättwil-Baden, Switzerland (corresponding e-mail: alexandre.oudalov@ch.abb.com)*
** *Power System Laboratory, ETH Zürich, CH-8092 Zürich, Switzerland (e-mail: {ulbig, andersson}@eeh.ee.ethz.ch)*

Abstract: Battery Energy Storage Systems (BESS) are very effective means of supporting system frequency by providing fast response to power imbalances in the grid. However, BESS are costly, and careful system design and operation strategies are needed in order to generate revenue for the system owner. We propose control strategies which will help to maintain BESS's State of Charge (SoC) in the optimal range and slow down battery aging significantly. A validation of these strategies using data from ENTSO-E (for the German regulation market) in Continental Europe and the PJM interconnection in the USA is presented in the results section.

1. INTRODUCTION

In recent years many countries have opened ancillary service markets, and system services such as frequency regulation have become commercial. After passing a technical pre-qualification process, suppliers may participate in the regulation market. BESS can be a very effective means of supporting system frequency. By charge or discharge, BESS can provide regulation power to the grid via power electronic inverters with very fast response time (<20 ms), making BESS a much better choice in terms of performance compared to traditional Pumped Hydro Storage (PHS) units. In Oudalov et al. [2006] and Mercier et al. [2009], BESS is shown to have a high value in supply frequency control power in utility scale applications.

One characteristic in providing frequency regulation is the inflexibility of operation. During the regulation period, units have to follow either self-measured system frequency deviations or control signals provided by the transmission system operator (TSO). Failure in signal following can result in payment reduction or disqualification of service. These signals are not guaranteed to be zero-mean and losses are inherent in BESS, in which case state of charge (SoC) restoration must be performed due to BESS's capacity limitation. Though increment in installation capacity provides BESS's with higher capability to sustain short-time deviations, over dimensioned BESS energy capacity may be too costly due to degradation. In battery degradation, part of the capacity fading occurs spontaneously (See Vetter et al. [2005]), therefore with the same control signal, a larger BESS will result in lower utilization of its battery cells. Thus BESS has to be reasonably sized, while certain control methods have to be used to restore and maintain BESS's SoC without creating large disturbance on the unit's operation point.

In Oudalov et al. [2007], a simple method is proposed to control SoC in primary frequency control, however this method does not grant BESS the ability to sustain large frequency deviations. Thus we propose control strategies which are more flexible and robust against worst-cases. Validations of these strategies using data from ENTSO-E (German market) in Continental Europe and PJM interconnection in the USA is presented in this paper. It starts by giving an overview of relevant regulation market backgrounds in Section II, followed by the proposed control strategies in Section III. The analysis methods are introduced in Section IV, and strategies validation results are presented in Section V. In the end, conclusions are given in Section VI.

2. REGULATORY BACKGROUND

2.1 Primary Control in ENTSO-E

In ENTSO-E, primary frequency control (PFC) describes the first tier of frequency control. Participating units provide a regulation power proportional to the deviation from nominal frequency. Full activation is at 200 mHz with a maximum delay of 30 seconds. A no-activation deadband of 20 mHz (±10 mHz) is allowed (see Rebours et al. [2007]). The tendering period in Germany is one week, and payment is only made with respect to the reserve power capacity.

2.2 Fast Regulation in PJM

In the PJM regulation market, the secondary control signal is split into a dynamic control signal (RegD) and a traditional control signal (RegA). RegD is the high-pass filtered part of the area control error (ACE), and RegA is the low-pass filtered part of ACE. RegD has a larger signal ramp rate and a smaller energy deviation compared to RegA, and is designed for fast-responding storage units (PJM [2012]).

PJM recently introduced the two-part offer policy in its regulation market. In this scheme, regulation units are paid by their regulation capability (reserve) as well as their

Copyright © 2014 IFAC

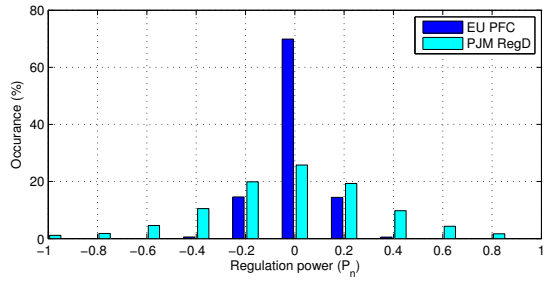

(a) Regulation power

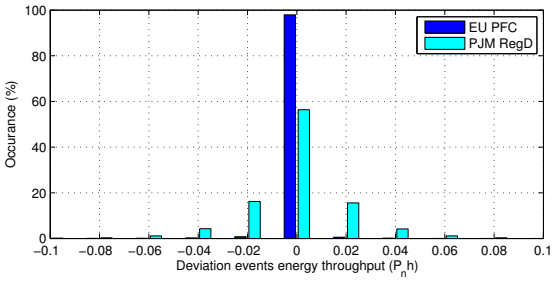

(b) Regulation energy throughput in one deviation event

Fig. 1. Comparison of PFC in EU and RegD in PJM.

performance in following regulation signals. The tender offer is divided into a capability offer and a performance offer, and the regulation credit is awarded based on the capability clearing price (RMCCP) and the performance clearing price (RMPCP). A regulation unit's output is evaluated with respect to the control signal it received in terms of correlation, delay, and precision. The result is recorded as performance score scaled between 0 to 1, and is used in market clearing as

$$\text{Regulation Credit} = \text{Capability} \cdot (\text{RMCCP} + \text{RMPCP} \cdot \text{Actual Mileage} \cdot \text{Actual Performance Score}) \quad , \qquad (1)$$

where Actual Mileage is the absolute sum of movement of the regulation signal during the payment period (details are explained in PJM [2012]). For the RegA signal the Mileage is normally about 5 to 6 ΔP_n per month, and for the RegD signal it is around 16 ΔP_n.

2.3 Regulation Signal Comparison

In Fig. 1, the PFC signal in ENTSO-E and RegD signal in PJM are compared in terms of power, and energy. Note that these two signals are not identical since they belong to different tiers in the ancillary service framework, while comparisons are made only to analyze their stresses on BESS operations. In Fig. 1a, the statistic of requested power is shown, and Fig. 1b shows the statistic of regulation energy throughput over one deviation event (starts when the regulation signal goes across zero point till it returns). The unit in both plots is in nominal power (P_n).

RegD signal shows a severer situation in either cases, with an average absolute regulation power of $0.27P_n$, while in PFC the average power is only $0.08P_n$. However due to the filtering mechanism, the highest deviation energy in RegD signal is limited to $0.23P_nh$, while in PFC there are several cases for which the energy deviation goes above $0.5P_nh$.

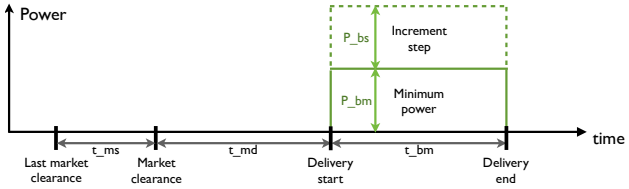

Fig. 2. Generalized intraday market regulations.

3. SOC CONTROL STRATEGIES

3.1 Intraday Bidding Control

To maintain BESS's SoC and ensure the regulation performance, a solution is presented by participating in the intraday energy market. In this method, market bids are determined according to the BESS's condition. Energy is purchased from the intraday market to charge up the battery if SoC is low, or sold if SoC is high. Upon power delivery, the operation point of BESS is set as

$$P_{ext} = P_{AS} + P_{bid}, \qquad (2)$$

where P_{ext} is the extracted power from BESS, P_{AS} is the power required by the regulation, and P_{bid} is the power delivered from/to the market. This allows the corrective control of SoC level while the following of the regulation signal can be undisturbed.

Intraday energy market allows a continuous trading of power contracts. Though market regulations vary with different operators, it can be generalized as following (a graph illustration is shown in Fig. 2):

- Market power is physically delivered with a certain delay (t_{md}) after the market clearance,
- A certain step time (t_{ms}) exists between one market clearance and the next one,
- Contract power values are required with a minimum absolute value (P_{bm}), and an increment step (P_{bs}),
- Contracts usually have a minimum duration (t_{bm}).

Based on the generalized market regulations, a proportional controller is designed to determine the value of power bids at each market clearance. With this method instant contract clearing is assumed. The duration of power contracts are always set to the minimum duration t_{bm}. At each trading action, an SoC prediction (σ_p) is made over the horizon ($t_{md} + t_{bm}/2$) to predict the SoC level at the middle of the expected delivery. Then the controller determines the value of the bid from the difference between the prediction and the reference SoC (σ_{ref}) as

$$P_{bid} = \frac{E_{BESS}}{t_p}(\sigma_{ref} - \sigma_p) \quad , \qquad (3)$$

where σ_{ref} is the reference SoC level, E_{BESS} is the energy size of the BESS, and t_p is the controller's time coefficient. t_p represents the time that the SoC can be restored to the reference level by the contracted power after the delivery starts, ignoring deviations taken place after the market clearance. Thus t_p should be chosen at least no smaller than the duration of the bid to avoid SoC exceeding the reference level. The result from the controller needs to be

floored (or capped if the result is negative) to the nearest allowed bidding power by the regulation market.

3.2 GM(1,1) SoC Predictor

In this work a SoC predictor based on grey system theory (See Wen [2004]) is developed to fulfill the prediction task in the intraday bidding control strategy. GM(1,1), or called "Grey Model First Order One Variable", is a time series forecasting model only applicable to non-negative data sets. For a given data set $X^{(0)}$ with a length of k samples

$$X^{(0)} = (x^{(0)}(1), x^{(0)}(2), \dots, x^{(0)}(k)) \quad , \tag{4}$$

the prediction $x_p^{(0)}$ over the horizon H at time step k is shown as

$$x_p^{(0)}(k+H) = [x^{(0)}(1) - \frac{b}{a}]e^{-a(k+H-1)}(1-e^a) \quad , \tag{5}$$

where a and b are model coefficients calculated from the input series $X^{(0)}$, methods are shown in Kayacan et al. [2010]. In Khalid and Savkin [2010], the GM(1,1) model is used to forecast short term (6 seconds) frequency variations. However to use the predictor in intraday bidding control, the prediction horizon is much larger (around one hour). Thus to achieve higher accuracy, SoC predictions are made directly using recorded SoC series. To use the GM(1,1) model for SoC prediction, the accumulated amount of energy delivered from or to the intraday market is recorded, and removed from the SoC profile (σ) to obtain an uncontrolled "raw" SoC profile (σ'), namely

$$\sigma'(k) = \sigma(k) - \sum_{i=1}^{k} P_{bid} t_s \quad , \tag{6}$$

where t_s is the sampling time of operation. σ' shows the natural variation of regulation energy throughput, and should be used for prediction in order to eliminate control effects. An offset δ_σ is added to σ' before prediction and removed from the result to avoid negative values. The prediction at time step k can be expressed as

$$\begin{aligned}\sigma_p(k+H) =& [\sigma'(k-H) + \delta_\sigma - \frac{b}{a}]e^{-a(2H)}(1-e^a) \\ & - \delta_\sigma + \sum_{i=1}^{k+H} P'_m t_s \quad ,\end{aligned} \tag{7}$$

in which a and b are calculated from the series $(\sigma'(k-H), \dots, \sigma(k))$ [1].

3.3 Averaging SoC Control

In some regulation markets, for example PJM, regulation units are not required to strictly follow control signals. In these cases more flexible control methods can be used to control BESS's SoC. In this work, a moving average control method (See Borsche et al. [2013]) is used. The method averages battery's net energy consumption over an averaging period (a) and set the working point (P_{WP}) of the battery accordingly after a certain delay (d). For time step k, this mechanism can be explained as

$$P_{WP}(k+d) = \frac{\sum_k^{j=k-a}(-P_{AS}(j) + P_{loss}(j))}{a} \quad , \tag{8}$$

where P_{AS} is the demand from ancillary services and P_{loss} is the power loss of the battery. Thus at time step $k+d$, the extracted (output) power (P_{ext}) from the battery will be

$$P_{ext}(k+d) = P_{AS}(k+d) + P_{WP}(k+d) \quad . \tag{9}$$

However, to be compatible with BESS's power and SoC limitation, this method is modified as

$$P_{WP}(k+d) = \frac{\sum_k^{j=k-a}(-P_{AS}^{lim}(j) + P_{loss}(j))}{a} \quad , \tag{10}$$

where P_{AS}^{lim} is the adjusted ancillary service demand power due to BESS's power and energy limitation, and can be calculated as

$$P_{AS}^{lim}(k) = P_{ext}^{lim}(k) - P_{WP}(k) \quad , \tag{11}$$

where P_{ext}^{lim} is the adjusted output power from the battery. P_{ext}^{lim} can be calculated first by capping P_{ext} with BESS's power limitation

$$P_{ext'}(P_{ext}) = \begin{cases} P_n & \text{if } P_{ext} > P_n \\ -P_n & \text{if } P_{ext} < -P_n \\ P_{ext} & \text{else} \end{cases} \quad , \tag{12}$$

and then the result is capped with BESS's SoC limitation ($\sigma^{up} \le \sigma \le \sigma^{down}$) to obtain P_{ext}^{lim}

$$P_{ext}^{lim}(\sigma, P_{ext'}) = \begin{cases} 0 & \text{if } \sigma > \sigma^{up} \text{ and } P_{ext'} < 0 \\ 0 & \text{if } \sigma < \sigma^{down} \text{ and } P_{ext'} > 0 \\ P_{ext'} & \text{else} \end{cases} \quad . \tag{13}$$

4. ANALYSIS METHOD

4.1 Degradation Model

To evaluate BESS's degradation cost, a linearized semi-empirical capacity degradation model developed based on Millner [2010] and experimental data is used. In the model, battery ageing life (L) is decoupled into cycling ageing (L_{cyc}) and calendar ageing (L_{cal}), plus the degradation damage already occurred in previous operations (L_{prev}). The model takes the SoC (σ) and cell temperature (T) series as well as the time duration (t_{faded}) of a BESS operation. The two series are processed using the rainflow cycle-counting algorithm (Downing and Socie [1982]) to count the number of cycles (N) as well as the SoC ($\boldsymbol{\sigma}$), Depth of Discharge (DoD, $\boldsymbol{\delta}$), and temperature ($\boldsymbol{T}$) of each counted cycle. The cycle counting results are used

[1] Various profile lengths are tested for prediction, the best result is achieved with profile length equal to prediction horizon

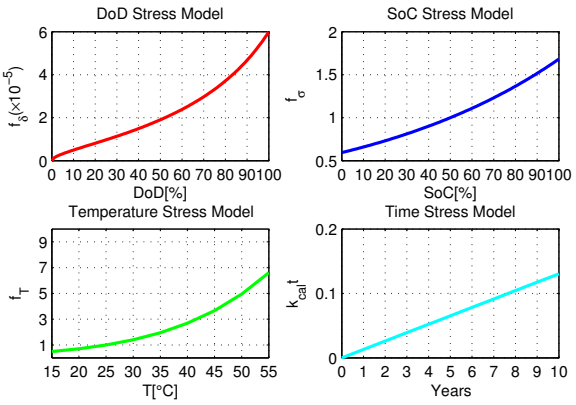

Fig. 3. Battery degradation impacts caused by DoD, SoC, temperature and ageing.

to evaluate the cycling damage, while t_{faded} as well as the profile average SoC ($\overline{\sigma}$) and temperature ($\overline{T}$) are used to calculate the calendar ageing, shown as

$$L = L_{cyc}(\boldsymbol{\sigma}, \boldsymbol{\delta}, \boldsymbol{T}, N) + L_{cal}(\overline{\sigma}, \overline{T}, t_{faded}) + L_{prev} \quad , \quad (14)$$

in which

$$L_{cyc} = \sum_{i=1}^{N} f_\delta(\delta_i) \cdot f_\sigma(\sigma_i) \cdot f_T(T_i) \quad , \quad (15)$$

and

$$L_{cal} = k_{cal} f_\sigma(\overline{\sigma}) f_T(\overline{T}) t \quad , \quad (16)$$

where k_{cal} is the calendar ageing coefficient, and f_δ, f_σ, f_T are stress factor models of DoD, SoC, and temperature, respectively (shown in Fig. 3).

4.2 Simulation Model

The simulation model is used to calculate the SoC variation during BESS operation simulation. The SoC is updated at each simulation time step as

$$\sigma(k+1) = \sigma(k) - \frac{It_s}{Q_{BESS}} \quad , \quad (17)$$

where I is the current extracted from the BESS, and Q_{BESS} is BESS's charge capacity (usually in Ah). Current offers a more accurate indication of SoC variation in batteries than output power, and can be calculated from a battery's efficiency model

$$V_{oc}(\sigma) I_{cell} = I_{cell}^2 R_o(\sigma, T, I_{cell}) + P_{ext} \quad , \quad (18)$$

where I_{cell} is the cell current, V_{oc} is the open circuit cell voltage, and R_o is cell inner resistance. All transient behaviors are ignored in this model. I_{cell} can be calculated from the number of parallel connected cells in BESS. V_{oc} and R_o are dynamic variables depending on cell's condition (SoC, temperature, charge/discharge), and models from Lam et al. [2011] are used in this work. When ignoring cell efficiency ($V_{oc} = V_{nom}, R_o = 0$), the simulation model can be simplified as

$$\sigma(k+1) = \sigma(k) - \frac{P_{ext} t_s}{E_{BESS}} \quad , \quad (19)$$

where E_{BESS} is BESS's energy capacity.

4.3 Pricing Setup

To analyze BESS's revenue in providing regulation services, first the BESS's cost is modeled as

- Lithium-ion battery cell price in 2012 was 800 \$/kWh, and is estimated to linearly decreases to 200 \$/kWh by 2032 [2] ,
- Lithium-ion battery cell end of life (EoL) = 80 % rated capacity,
- BESS equipment cost except cells (including construction, converters, cooling system, etc): 1.2 M\$ per MW, 20 years lifespan,
- Electricity cost: 50 \$/MWh.

In which after the installation of the BESS, only the battery cells are replaced once they reached the 80% EoL, until the entire system reaches the 20 years lifetime. Lithium-ion battery systems require no maintenance, and only cooling is considered. The cooling cost is modeled assuming all generated heating energies (E_{heat}) are neutralized by the cooling system with a cooling power efficiency of 50%, shown as

$$\text{Cooling Cost} = \frac{1}{0.5} \cdot E_{heat} \cdot 50\$/\text{MWh} \quad . \quad (20)$$

On the market side, the intraday contract price is fixed at 50 \$/MWh (same for selling and buying). The PFC payment price in EU is set to 20 \$/MW·h, averaged from regelleistung.net [3] . In the PJM regulation market, the real time recorded RMCCP and RMPCP price series are used. The average value of RMCCP is 20 \$/MW·h, and for RMPCP the value is 6 \$/ΔMW.

5. SIMULATION RESULTS

5.1 ENTSO-E Case

BESS PFC simulations are performed with the intraday bidding controller and the GM(1,1) SoC predictor. The time coefficient t_p is set to $max((t_{md} + t_{bm})/2, t_{bm})$ to increase controller's tolerance on large prediction errors due to the high prediction horizon. Simplified German intraday market policy ($t_{md} = 45\,\text{m}$, $t_{ms} = 15\,\text{m}$, $t_{bm} = 15\,\text{m}$) with 100% bid success rate is used, and the minimum bidding value is set to 100 kWh, scaled 10 times down from the 1 MW requirement in the German market. The frequency profile from Feb 01, 2011 to Dec 30, 2011 is used, and BESS temperature is assumed to be a constant $25°C$.

First, regulation energy throughput simulation is performed. An example of the simulation result is shown in

[2] Source: Bloomberg New Energy Finance (`bnef.com/InsightDownload/7028/pdf/`)
[3] The transparency platform of the German transmission system operators (`www.regelleistung.net`)

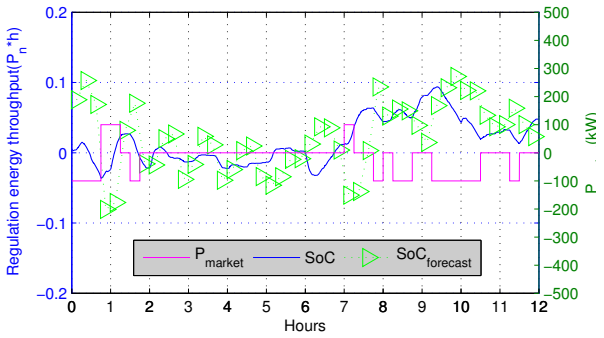

Fig. 4. Example of regulation energy throughput simulation with market SoC control and GM(1,1) predictor.

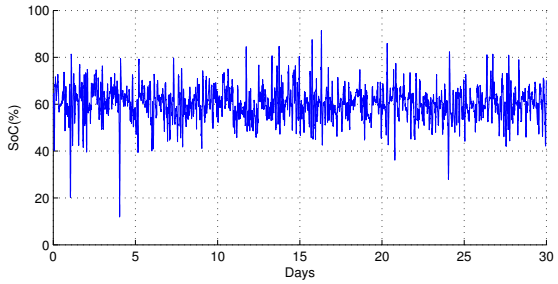

Fig. 5. SoC in PFC simulation with battery efficiency ($0.6P_nh$ size, profile: 2011/11/01 - 2011/11/30).

Fig. 4, in which variation of regulation energy, energy prediction and the intraday market power are included. The minimal energy size of the battery obtained from the yearly simulation is 0.45 P_nh, corresponding to 0.45 MWh with 1 MW PFC reserve.

The energy throughput simulation is also performed with different market regulations. It is assumed in the simulations that the duration of power contracts is always equal to the period of market clearance ($t_{ms} \equiv t_{bm}$). The round-trip battery efficiency is $\eta^2 = 0.9$, and SoC level is controlled between 10% to 90%. The resulting BESS sizes with respect to different market delays and contract durations is shown in Fig. 6. The fact that the BESS size increases linearly with larger contract duration is due to that BESS is not able to quickly adjust its operation point and thus has to sustain longer deviations. The BESS size also increases with market power delay, which is mainly due to the larger errors in the SoC prediction, while in the simulation with ideal forecast the BESS size results showed no dependences on the market delay.

Simulation with battery efficiency model is performed for providing 1MW reserve with the minimal battery size of 0.6 MWh. During the simulation, 261.6 MWh energy is discharged from the BESS, while 264.9 MWh is charged, and 3.3 MWh of heat is generated by the BESS. 144.3 MWh energy is purchased from the intraday market, and 136.0 MWh is sold, giving a net energy flow of 8.6 MWh. All power outputs are below the 1 MW system rating throughout all simulations. The resulting linearized capacity degradation is 3.43%, corresponding to a loss of 21 kWh in battery cells. The SoC simulation result of November, in which the largest SoC deviation happened, is shown in Fig. 5.

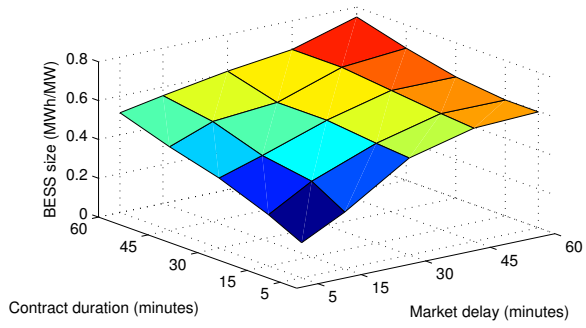

Fig. 6. BESS energy capacity with various intraday market regulations in PFC.

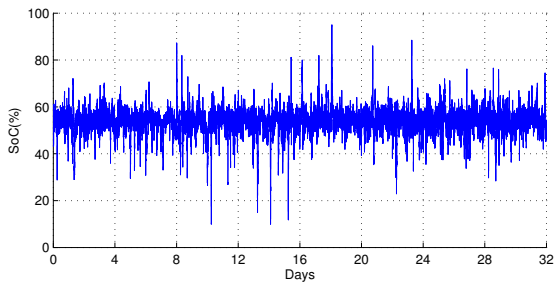

Fig. 7. SoC in PJM simulation with battery efficiency ($0.6P_nh$ size, profile: 2012/12/18 - 2013/01/18).

5.2 PJM Interconnection Case

In the PJM RegD case, simulations are performed with the battery efficiency model and constant BESS temperature ($25°C$). The moving average delay d is fixed at 15 minutes, meaning compensating operations are made at secondary control timescale. The averaging period a includes 5, 15, 60, or 120 minutes, and for each value of a a simulation is performed with an appropriate BESS size. The regulation capability is set to 1 MW. The RegD profile from Dec 18, 2012 to Jan 18, 2013 is used, with a total duration of 32 days, and the average signal mileage is 16.9. The SoC result of the simulation with 0.6 MWh/MW BESS size (a = 60 minutes) is shown in Fig. 7.

At each simulation, the linearized capacity degradation is estimated. The performance score and the payment credit are calculated hourly and their average is shown in the following table as well as other parameters.

Table 1. PJM RegD Simulation Results (20121218-20130118)

	Case 1	Case 2	Case 3	Case 4
BESS Size (MWh/MW)	0.20	0.33	0.60	1.00
Avg. period (minutes)	5	15	60	120
Performance Score	0.9	0.96	0.99	0.99
Capacity Degradation(%)	2.77	1.66	1.14	0.84
Heating Energy(MWh)	16.81	8.07	3.37	2.50
Average Credit($/h)	113	120	123	123

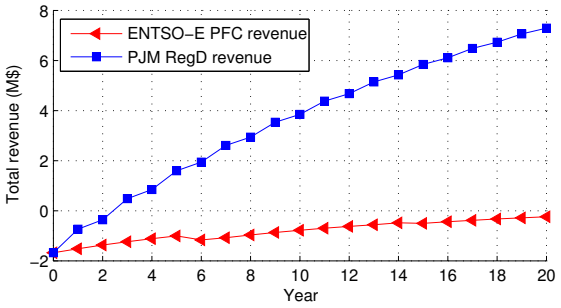

Fig. 8. 20 years NPV revenue comparison of a 0.6 MWh BESS providing PFC in ENTSO-E and RegD in PJM.

The results show a generally good regulation performance with a score between 0.9 to 0.99, while the average performance score in the PJM regulation market was around 0.7 to 0.8 [4]. With a shorter averaging period, the BESS adjusts its operating point more aggressively and thus results in a lower performance score. And the degradation is more severe due to smaller battery size and more intense operation.

5.3 Revenue Analysis

Net present value (NPV) revenue analysis is performed for both simulation cases with the established pricing and a discount rate of 6%. The BESS size is 0.6 MWh and the regulation capability is 1 MW in both cases. Regulation payments are assumed to be proportional to BESS's state of health (SoH), while the cost includes installation, cell replacement, cooling and intraday market transactions. Based on the simulation results, battery cells are replaced every 7 years in the ENTSO-E PFC case, and every 2 years in the PJM RegD case.

The result shows a much more profitable situation in providing RegD regulation in PJM, with a system payback time in 3 years, while the ENTSO-E PFC case is shown to not be profitable. This is mainly due to the different levels of reserve capacity payments. Regulation payments from PJM are roughly 6 times higher compared to PFC in ENTSO-E.

6. CONCLUSION

In this paper, control strategies aiming at maintaining BESS's SoC level in frequency regulation applications are presented. An intraday market based SoC control method is proposed, with which BESS's operation can be undisturbed when its SoC being restored, and a GM(1,1) based SoC predictor is developed to offer forecasts for the controller. An averaging SoC control method is shown as an alternative choice when certain flexibilities are allowed in providing regulation.

Regulation simulations are performed for providing regulation in Germany and in PJM, USA. With the proposed control strategies, a BESS size of $0.6P_nh$ can be enough for both cases. By modeling the degradation as well as other cost factors, NPV revenue analysis shows a much more profitable case in PJM compared to Germany. This result implies that to introduce BESS into existing ancillary service frameworks, regulation market polices must be adjusted to make use of the fast responding characteristic of BESS, and to sufficiently compensate the cell degradation cost which are still quite high at present.

[4] Source: `http://www.pjm.com/markets-and-operations/ancillary-services/mkt-based-regulation.aspx` (last accessed: 2013-08-21)

REFERENCES

PJM Manual 12: Balancing Operations, 2012. URL `http://pjm.com/~/media/documents/manuals/m12.ashx`.

Theodor Borsche, Andreas Ulbig, Michael Koller, and Göran Andersson. Power and energy capacity requirements of storages providing frequency control reserves. In *Power and Energy Society (PES) General Meeting, 2013 IEEE Vancouver*, 2013.

Stephen D Downing and DF Socie. Simple rainflow counting algorithms. *International Journal of Fatigue*, 4(1):31–40, 1982.

Erdal Kayacan, Baris Ulutas, and Okyay Kaynak. Grey system theory-based models in time series prediction. *Expert Systems with Applications*, 37(2):1784–1789, 2010.

Muhammad Khalid and Andrey V Savkin. Model predictive control based efficient operation of battery energy storage system for primary frequency control. In *Control Automation Robotics & Vision (ICARCV), 2010 11th International Conference on*, pages 2248–2252. IEEE, 2010.

Long Lam, P. Bauer, and E. Kelder. A practical circuit-based model for li-ion battery cells in electric vehicle applications. In *Telecommunications Energy Conference (INTELEC), 2011 IEEE 33rd International*, pages 1–9, 2011. doi: 10.1109/INTLEC.2011.6099803.

Pascal Mercier, Rachid Cherkaoui, and Alexandre Oudalov. Optimizing a battery energy storage system for frequency control application in an isolated power system. *Power Systems, IEEE Transactions on*, 24(3): 1469–1477, 2009.

A. Millner. Modeling lithium ion battery degradation in electric vehicles. In *Innovative Technologies for an Efficient and Reliable Electricity Supply (CITRES), 2010 IEEE Conference on*, pages 349–356, 2010. doi: 10.1109/CITRES.2010.5619782.

A Oudalov, D Chartouni, C Ohler, and G Linhofer. Value analysis of battery energy storage applications in power systems. In *Power Systems Conference and Exposition, 2006. PSCE'06. 2006 IEEE PES*, pages 2206–2211. IEEE, 2006.

Alexandre Oudalov, Daniel Chartouni, and Christian Ohler. Optimizing a battery energy storage system for primary frequency control. *Power Systems, IEEE Transactions on*, 22(3):1259–1266, 2007.

Yann G Rebours, Daniel S Kirschen, Marc Trotignon, and Sébastien Rossignol. A survey of frequency and voltage control ancillary servicespart i: Technical features. *Power Systems, IEEE Transactions on*, 22(1):350–357, 2007.

J. Vetter, P. Novk, M.R. Wagner, C. Veit, K.-C. Mller, J.O. Besenhard, M. Winter, M. Wohlfahrt-Mehrens, C. Vogler, and A. Hammouche. Ageing mechanisms in lithium-ion batteries. *Journal of Power Sources*, 147 (12):269 – 281, 2005. ISSN 0378-7753.

Kun-Li Wen. *Grey systems: modeling and prediction*. Yang's Scientific Research Institute, 2004.